MECHANISMS OF INITIAL SINTERING OF A FINE ALUMINA POWDER

S. Raman, R. Doremus, R. German

JOURNAL DE PHYSIQUE
Colloque C1, supplément au n°2, Tome 47, février 1986 page C1-225

MECHANISMS OF INITIAL SINTERING OF A FINE ALUMINA POWDER

S.V. RAMAN*, R.H. DOREMUS and R.M. GERMAN

Dept. of Materials Engineering, Rensselaer Polytechnic Institute, Troy, N.Y. 12181, U.S.A.

Résumé - Nous avons étudié par microscopie électronique et diffraction des rayons X le mécanisme du frittage de l'alumine. La transformation de l'alumine gamma en alumine alpha influence la vitesse de frittage. Cette transformation semble entraîner la déformation plastique de l'alumine. L'énergie d'activation que l'on mesure pour le frittage de la poudre d'alumine alpha est comparable à celle de la diffusion d'oxygène dans les joints de grains.

Abstract - The mechanism of initial sintering of alumina was explored by electron microscopy and X-ray diffraction. The transformation of gamma to alpha alumina influenced sintering behavior. This transformation appears to involve plastic deformation in the alumina. Sintering of fine alpha alumina powder directly occurs with an activation energy close to that of grain boundary diffusion of oxygen.

I - INTRODUCTION

The sintering of alumina has been widely studied because it is an important high temperature material and was thought to be relatively simple. However, sintering of alumina is influenced strongly by the size, morphology and structure of the starting powder, and is complicated by transformations of metastable phases to the stable alpha phase. Very fine ($\simeq$100 A^{o} diameter) agglomerated gamma alumina powder (Fig. 1) showed a low activation energy for sintering at 1200°C to 1400°C (72 to 82 kj/mol), and sintered more rapidly than alpha powder /1/. The surface area reduction during sintering at 1200 to 1400°C was examined with the models of German and Munir /2/ and the time exponent was that expected for plastic flow. The model of Young and Cutler /3/ when compared with shrinkage results was also consistent with plastic flow. The literature contains conflicting reports /4,5/ as to the relative importance of plastic flow in the sintering of undoped alumina.

In this paper the previous results /1/ have been extended through selected area electron diffraction and electron microscopy, to follow the influence of diffusion mechanism and phase transformation on the evolution of sintered microstructure.

II - EXPERIMENTAL METHODS

In the previous study /1/ the sintering of gamma and alpha alumina powders was examined by isothermal and constant heating rate experiments. In the present work these sintered pellets have been investigated by transmission electron microscopy (TEM) and selected area electron diffraction (SAD). For TEM samples the pellets were ground to 20 to 50 micron thickness, held in the sample holder between tantalum plates and ion milled on both surfaces with 6.5KV Ar ions. The milling time varied from 60 to 160 hours depending on the density of the pellets. Denser pellets required longer time. The ion milled foils were carbon coated and examined under bright field condition at an accelerating voltage of 100KV and 1000KV.

*Present address : Brookhaven National Laboratory, Upton, N.Y. 11973, U.S.A.

III - EXPERIMENTAL RESULTS

Figures 2 to 8 show transmission electron bright field images and associated selected area electron diffraction patterns of pellets sintered for two hours at

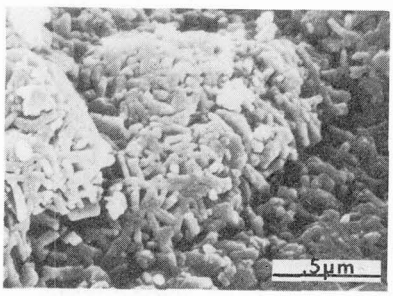

Fig. 1 Scanning electron micrograph of gamma alumina green pellet.

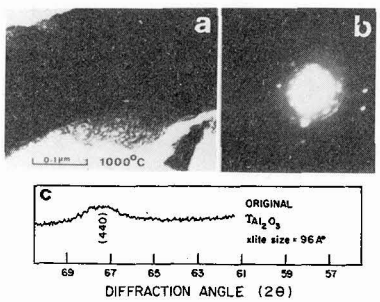

Fig. 2 (a) TEM micrograph of a rodlet of green gamma alumina observed in figure 1 (b) the associated SAD pattern (100KV) (c) X-ray diffraction pattern of gamma alumina powder.

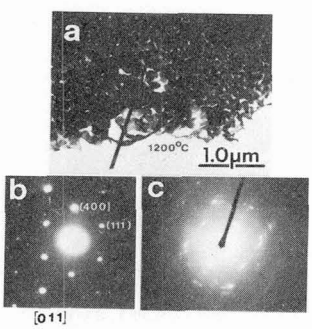

Fig.3a Micrograph of sintered pellet at 1200°C (100KV), (b) FCC SAD pattern of .3 gamma grain, (c) polycrystalline deformed diffraction pattern of matrix.

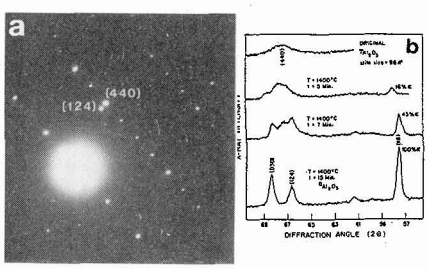

Fig. 4 (a) Double diffraction from coexistence of gamma and alpha phase at 1200°C (100KV) (b) The quenchable transformation of gamma to alpha phase is shown by X-ray powder pattern of heat treated powders at 1400°C.

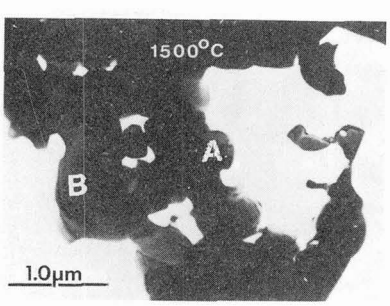

Fig. 5 Clusters of alpha grains (region A) are in the process of coalescence at 1500°C. and the coalesced grain (region B) is bound by curved grain boundaries. (100KV)

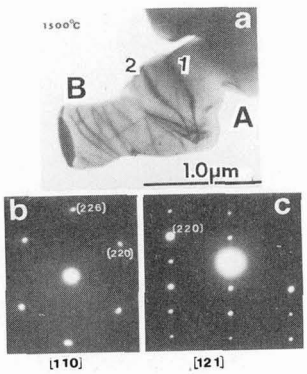

Fig. 6 (a) Grains A and B occur juxtaposed against a normal grain boundary, 1 and 2 are the dislocation images on (110) foil plane. (b) and (c) are SAD patterns of grains A and B. (100KV)

different temperatures. The green state (Fig. 2a) consisted of fine spherical gamma alumina particles that compose the agglomerated rodlets observed in figure 1. The particle size appears to be in the range of 60 to 100 A^{o}. Consistent with the fine particle size are polycrystalline SAD rings (Fig. 2b) and the broad (440) X-ray reflection (Fig. 2c). After sintering at 1200°C the particles were about 1000 A^{o} in size and formed interconnected chains (Fig. 3a). Their SAD pattern had streaks and deformed spots (Fig. 3c). Where a grain as large as 0.3microns was encountered by the beam a single crystal diffraction pattern characteristic of an FCC (011) lattice of gamma alumina was obtained (Fig. 3b). With appropriate specimen tilting double diffraction spots (Fig. 4a) characterisic of a mixture of gamma and alpha phases were evident. The relationships between these two reflections of (440) and (124) were also studied after sintering at a higher temperature of 1400°C (Fig. 4b) /1/. A distribution of grain sizes was evident at a higher sintering temperature of 1500°C. Alpha grains 0.3micron in size clustered (region A of Fig. 5) and eventually grew into larger grains (region B of Fig. 5). At a higher magnification a thin section of this sample showed line defects amidst bend contours. The line defects in figure 6a were identified by their immobility with specimen tilting. Thus the images marked 1 and 2 in figure 6a could be distinguished from bend contours, because the scattering factor arising from atomic displacements superimposes on the normal scattering process during specimen tilting. The single crystal SAD patterns are characteristic of (110) and (121) foil orientations (Figs. 6b and 6c) and point to the presence of a normal grain boundary between A and B grains of figure 6a.

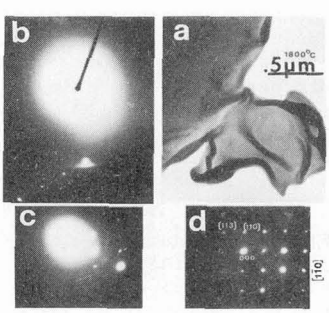

Fig. 7 (a) Micrographs of the pellet sintered at 1800°C. The 1000A^{o} diffuse bands are like extended dislocation images, (b) the SAD pattern of the diffuse band in the centre of the foil is made of deformed diffraction spots, (c) upon specimen tilting diffraction streaks originate from the same region, (d) the clear region of the foil reveals a normal SAD pattern of unstrained alpha alumina (100KV).

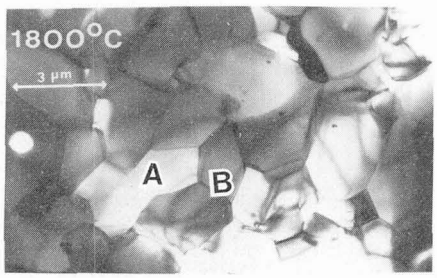

Fig. 8 Microstructural mosaic at 1800°C. (1000KV)

After sintering at 1800°C diffuse bands were observed within and around the thin foil (Fig. 7a). The diffraction spots appear deformed (Fig. 7b) within the region of the diffuse band and are normal in other regions (Fig.7d). When the specimen was tilted the deformed nature of the diffraction persisted in the form of streaks within the diffuse band (Fig. 7c). In the high voltage electron microscope, at an operating voltage of 1000KV, a larger area of the microstructure was visible (Fig. 8). There were pores at grain boundaries, and some pores were inside grains. The microstructure was predominantly dense.

IV - DISCUSSION

Defect Features The two dark images marked 1 and 2 on (110) foil plane (Fig. 6a) are like dislocation images cited by Morrissey and Carter /6/. The diffuse bands in figure 7a are 1000A° wide and are composed of two dark lines separated by diffuse regions. The electron diffraction of these images is composed of elongated diffraction spots. Discussions in the literature /7,8/ attribute shape changes of electron diffraction spots to the strain fields associated with dislocations and stacking faults. It is also of interest to note that Kingery et al. /9/ have described formation of extended dislocations in alumina by mobility of Al and O ions through partial paths. Considering the width of 1000A° for the images shown in Fig. 7a it is likely that the two embedded dark lines are partial dislocations separated by unresolved diffuse regions of stacking faults. The dislocation structure observed in this work is unlike the ones shown in deformed single Sapphire crystals /10,11/ and alumina whiskers /12/ where high density of dislocations were reported on the basal plane in the form of curvilinear lines, loops and dipoles. Dislocation images in sintered pure polycrystalline alumina have not been cited in detail, though discussions have favoured their importance in sintering /5,13,14/. Possibly their presence in sintered alumina is related to the mode of particle preparation, size and phase; and mechanism of dislocation motion during sintering and annealing. The low density of dislocations observed in the present work could be due to long anneal time of two hours that the samples were subjected to at the sintering temperatures. The discrepency in the image shape between the present micrograph and those reported by Barber and Tighe /10/. Pletka et al. /11/, and Kotchick and Tressler /15/ may be related to differences in the crystallographic orientation of the foil plane and motion of dislocations by climb mechanism. In support of the latter is the similarity between the dislocation image of (110) foil (Fig. 6a) and that reported by Morrissey and Carter /6/.

Significance of Activation Energies The kinetics of surface area reduction, in response to thermal stress induced by isothermal heat treatment of the powder enabled calculation of mechanism characteristic exponent /1/. Its value was 1.07 for gamma alumina, which suggested plastic flow with an activation energy of 82 kj/mol. A similar activation energy of 72 kj/mol was obtained under a near absence of thermal stress (Fig. 9). In this case the thermal driving force for stress induced

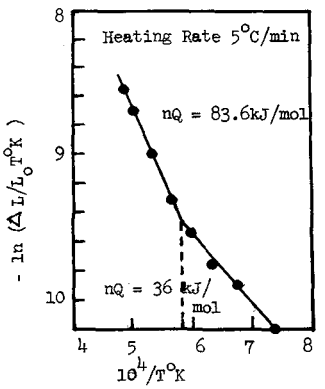

Fig. 9 Integral plot of shrinkage vs. temperature.

motion had been minimized by bringing the sample to sintering temperature at a low constant heating rate of 5°C/min. These activation energies resulted from volume diffusion at lower temperatures of 1000°C to 1400°C . Following the arguments presented by Weertman /16,17/ on similarity of activation energy between that for steady state creep and self diffusion, a dislocation climb mechanism was invoked /1/. It is supported in this work by the TEM image of dislocations. Above 1400°C the activation energy is 250 kj/mol for grain boundary diffusion. When compared to published reports /3,9,18,19,20/ these activation energies for both volume and grain boundary diffusion are significantly low and point to rapid sintering kinetics. An immediate cause for this difference was suspected to be related to the process of phase transformation and lattice metastability of the fine gamma alumina powder. That this indeed was the cause became evident from the sintering of alpha particles that were derived from gamma alumina powder through phase transformation (Fig. 4b). Pellets of these particles compacted under identical conditions (25%th. green density) sintered with an activation energy of 441 kj/mol /1/. This value is characteristic of oxygen grain boundary diffusion by Coble creep mechanism /20/. For these pellets grain boundary diffusion commences at a lower temperature of 1000°C owing to a larger average size of 200A° for alpha particles.

Microstructural Changes The transmission electron micrograph (Fig.2) coupled with continuous increase in shrinkage rate /1/ prior to phase transformation is in agreement with monodisperse size distribution for gamma alumina powder. However, heterogeneities in the size are introduced in the course of sintering as the pellet evolves to a density of 92%th. at 1800°C starting from a green value of 25%th. Initially the gamma particles were noted to grow to an average size of .3micron and then transform to a relatively finer .1 micron sized metastable alpha particles (Fig. 3). These particles in turn partly grow in accordance with Greskovich and Lay's mechanism /21/ and partly by lattice coalescence. Evidence for the latter mechanism is shown by the formation of an elongated grain in the microstructure of fig. 8. The abnormal size for this grain has probably resulted from the elimination of grain boundary that might have originally existed across the region marked A in the micrograph (Fig. 8). Another similar elongated grain could be conceived if the grain boundary marked B could be eliminated from the adjacent grains. Lattice coalescence would lead to grain boundary elimination if the adjacent grains were mutually rotated or moved such that the lattice elements of the grain boundary and the original lattice /22,23/ became identical. A very low concentration of pores in the entire microstructure (Fig. 8) and an overall interlocked granular mosaic suggest that the pores have been squeezed out by the movement of grains. Thus, although the microstructure appears 99% dense, the density of the pellet is only 92%th. This leads to the belief that immobile pores occur coalesced and clustered in some other parts of the pellet.

REFERENCES

/1/ Raman, S.V., Doremus, R.H. and German, R.M., in: Sintering and Heterogeneous Catalysis, vol. 16. G.C. Kuczynski, A.E. Miller and G.A. Sargent, eds. Plenum Press, (1984) 253.
/2/ German, R.M. and Munir, Z.A., J. Am. Ceram. Soc. 59 (1975) 379.
/3/ Young W.S. and Cutler, U.B., J. Am. Ceram. Soc. 53 (1970) 659.
/4/ Dynys J.M., Coble, R.L., Coblenz, W.S. and Cannon, R.M., in: Sintering and Heterogeneous Catalysis, vol . 15, G.C. Kuczynski, ed. Plenum Press, (1981) 391.
/5/ Morgan, C.S. and Tennery, V.J., in: Sintering and Heterogeneous Catalysis, vol. 15, G.C. Kuczynski, Ed. Plenum Press, (1981) 206.
/6/ Morrissey, K.J. and Carter, C.B., in: Character of Grain Boundaries, M.F. Yan, and A.H. Heuer, eds. (1983) 85.

/7/ Williame, J., Delavignette, P., Gevers, R. and Amelinckz, S., Phys. Stat. Sol. 17 (1966) K173.
/8/ Carter, C.B., Kohlstedt, D.L. and Sass, S.L., J. Am. Ceram. Soc. 63 (1980) 623.
/9/ Kingery, W.D., Bowen, H.K. and Uhlmann, D.R., John Wiley and Sons, (1976) 1032.
/10/ Barber, D.J. and Tighe, N.J., Phil Mag. (1966) 531.
/11/ Pletka, B.J., Mitchell, T.E. and Heuer, A.H., J. Am. Ceram. Soc. 57 (1974) 388.
/12/ Dragsdorf, R.D. and Webb, W.W., J. Appl. Phys. 29 (1958) 817.
/13/ Walker, F.R., J. Am. Ceram. Soc. 38 (1955) 187.
/14/ Ogbuji, L., Mitchell, T.E. and Heuer, A.H., in: Sintering and Catalysis, vol15, G.C. Kuczynski ed. Plenum Press, (1981) 305.
/15/ Kotchick, D.M. and Tressler, R.E., J. Am. Ceram. Soc. 63 (1980) 429.
/16/ Weertman, J., J. Appl. Phys. 26 (1955) 1213.
/17/ Weertman, J., J. Appl. Phys. 28 (1955) 362.
/18/ Oishi, Y. and Kingery, W.D., J. Chem. Phys. 33 (1960) 480.
/19/ Paladino, A.E. and Kingery, W.D., J. Chem. Phys. 37 (1962) 957.
/20/ Lessing, P.A. and Gordon, R.J., J. Mat. Sci. 12 (1977) 2291.
/21/ Greskovich, C., and Lay, K.W., J. Am. Ceram. Soc. 55 (1972) 142.
/22/ Brandon, D.C., Ralph, B., Ranganathan and Wald. M.S., Acta. Metal. 12 (1964)813.
/23/ Bollman, W. Phil. Mag. 16 (1967) 363.